TECHNICAL WORKING PAPER SERIES

AN EFFICIENT GENERALIZED DISCRETE-TIME APPROACH TO POISSON-GAUSSIAN BOND OPTION PRICING IN THE HEATH-JARROW-MORTON MODEL

Sanjiv Ranjan Das

Technical Working Paper 212

NATIONAL BUREAU OF ECONOMIC RESEARCH
1050 Massachusetts Avenue
Cambridge, MA 02138
June 1997

I would like to thank Kerry Back, Robert Bliss, Dilip Madan, Robert Merton, Pratap Sondhi, Peter Tufano, participants at the Financial Management Association Meetings 1996, and especially Chandranath Gunjal and Rangarajan Sundaram for valuable suggestions. This paper is part of NBER's research program in Asset Pricing. Any opinions expressed are those of the author and not those of the National Bureau of Economic Research.

An Efficient Generalized Discrete-Time Approach
to Poisson-Gaussian Bond Option Pricing in the
Heath-Jarrow-Morton Model
Sanjiv Ranjan Das
NBER Technical Working Paper No. 212
June 1997
JEL Nos. G13, C63
Asset Pricing

ABSTRACT

Term structure models employing Poisson-Gaussian processes may be used to accommodate the observed skewness and kurtosis of interest rates. This paper extends the discrete-time, pure-Gaussian version of the Heath-Jarrow-Morton model to the pricing of American-type bond options when the underlying term structure of interest rates follows a Poisson-Gaussian process. The Poisson-Gaussian process is specified using a hexanomial tree (six nodes emanating from each node), and the tree is shown to be recombining. The scheme is parsimonious and convergent. This model extends the class of HJM models by (i) introducing a more generalized volatility specification than has been used so far, and (ii) inducting jumps, yet retaining lattice recombination, thus making the model useful for practical applications.

Sanjiv Ranjan Das
Graduate School of Business Administration
Morgan Hall
Harvard University
Soldiers Field Road
Boston, MA 02163
and NBER
sdas@hbs.edu

1 Introduction

This paper develops a model for the pricing of American-type interest rate options when interest rates follow Poisson-Gaussian processes.[1] This model incorporates the effects of skewness and kurtosis in the distribution of interest rates on bond option prices. The paper advances the existing literature on bond option pricing in two broad ways. First, it extends existing pure-Gaussian models for American-type bond options to pricing under Poisson-Gaussian processes in the Heath-Jarrow-Morton [23] framework. Second, it enables skewness and kurtosis effects to be captured in the pricing of interest rate derivative securities.

The term structure of interest rates has been modelled extensively using primarily pure Gaussian models.[2] Recent empirical work[3] shows that models which accommodate skewness and kurtosis (such as stochastic volatility models and jump diffusion models) appear to fit the time series of interest rates better than pure Gaussian-type models. Changes in interest rates empirically evidence reasonable levels of skewness and kurtosis. Table 1 presents descriptive statistics for the one-month Treasury bill sampled at different frequencies. Clearly, a reasonable amount of skewness and kurtosis exists.

Skewness and kurtosis affect option values and the shape of the term structure (see Das [15]). Kurtosis results in fat-tailed distributions, which produce the well known 'smile' effect, where options which are away from the money trade at higher prices than those which are at the money.[4] Skewness results in an asymmetric interest rate distribution, which often makes it difficult for symmetric stochastic processes to fit both out-of-the-money calls and puts. If one is fit well, then the other will usually not match existing parameter choices, producing a one-sided 'smile' or a 'smirk'. In this paper, using two additional parameters, options can be priced to be consistent with an arbitrary range of distributional shapes providing for consistency with both skewness and kurtosis.

In recent times, lattice based models have been developed to accommodate the smile

[1] We employ the term 'Poisson-Gaussian' here to denote the discrete time analog to continuous time jump diffusion processes.

[2] See for example, the papers by Vasicek, [35], Cox-Ingersoll-Ross [13], and Heath-Jarrow-Morton [23], Amin and Jarrow [3], and Amin and Bodurtha [6] amongst several others.

[3] See Chan, Karolyi, Longstaff and Sanders [12], Brenner, Harjes and Kroner [10], Das [15], Heston [24] and Ait-Sahalia [1].

[4] The 'smile' is the plot of implied volatilities from a range of options of the same maturity across different strike prices. It is noticed that the options at-the-money seem to trade at the lowest implied volatilities, and the in-the-money and out-of-the-money options trade at higher volatilities. Since the options are all written on the same underlying variable, there should be no plausible reason for this, other than the fact that the model is inexact. Since the observed distribution of interest rates has fatter tails than that assumed by a pure-Gaussian model, such an effect is intuitively obvious. When plotted against the strike price, the graph of implied volatilities appears u-shaped as a 'smile'. Hence the terminology. Using the same visual logic, a one-sided smile is called a 'smirk'!

(Dupire [20], Derman and Kani. [17] and Rubinstein [33]). These models adjust the drift of the stochastic process on the lattice so as to exactly fit option prices for a range of moneyness and maturity characteristics. In contrast, this paper does not 'fit the smile'; instead, it introduces explicit parameters for skewness and kurtosis which can be tuned to capture the smile effect. This has the advantage of (i) being parsimonious, and (ii) has fewer computational complexities than algorithms which fit the smile.[5]

Apart from smile fitting methods, two alternative modelling approaches have been pursued: generalized volatility models, and Poisson-Gaussian models. This paper provides a model encompassing both approaches. Generalized volatility models allow volatility to take on some general form (deterministic in time or even stochastic), thus providing the desired levels of skewness and kurtosis. (Amin and Morton [5]) undertake an extensive empirical investigation of a class of these models). While these generalized volatility models are more malleable from the modelling standpoint, Poisson-Gaussian models reflect better the fact that kurtosis in the data increases as the sampling interval decreases. The manner in which kurtosis changes with the time interval between two observed interest rates distinguishes generalized volatility models from Poisson-Gaussian models. With diffusion based Markovian models (see Carverhill [11]. and Ritchken and Sankarasubramanian [32]), leptokurtosis is achieved, but usually decreases with the sampling interval, since the volatility of volatility has less effect as the time interval shrinks, which is contrary to empirical features of the data.[6] In Table 1, the kurtosis of changes in interest rates increases when the data is sampled daily instead of monthly. Moreover, interest rates often display discontinuous behavior, partly on account of the discrete changes the Federal Reserve makes in the short term interest rate. Modelling of the term structure using a Poisson-Gaussian process captures these market features better, because with these processes, the variance shrinks with the time interval, yet the size of the jumps remains the same, enhancing kurtosis, which is the relative size of the outliers to the variance of the process. Empirical evidence in Das [15] strongly supports the Poisson-Gaussian set of processes over stochastic volatility forms.

Previous work has attempted to handle skewness and kurtosis effects. Models of the interest rate where Poisson-Gaussian processes are employed have resulted in closed-form expressions for bond prices. as in Ahn & Thompson [7], Shirakawa [34], and Naik & Lee [31]. Other approaches using gamma processes were initiated by Heston [24]. Analytical solutions for European bond options under Poisson-Gaussian processes have also been developed by Shirakawa [34] and Naik & Lee [31]. As such, no closed form expressions for interest rate options of an American-type exist, and these have to be solved numerically. While several

[5]Fitting the smile is numerically intensive for equity options and is likely to be more so for interest rate options.

[6]Practitioners demonstrate evidence of this all the time when they assume that volatility is effectively constant for short maturity options.

approaches exist for the numerical solution of the American bond option pricing problem in the case of pure Gaussian processes (Ho & Lee [25], Heath-Jarrow-Morton [23], Brennan & Schwartz [9]), no solution has yet been available for the numerical solution of the American bond option pricing problem under Poisson-Gaussian processes. Das [16] offers one such approach using a modified finite-differencing scheme. In contrast, in this paper, a tree based scheme for the pricing of American options is provided. This paper presents a simple and efficient approach to pricing American-type interest rate derivatives when the underlying term structure of interest rates undergoes changes that are of both the continuous and discontinuous type ,i.e., a Poisson-Gaussian process.

The model employs a new lattice approach for the pricing of Poisson-Gaussian process based interest rate derivatives. Unlike pure-Gaussian processes, Poisson-Gaussian processes are not easily represented on a tree. In this paper, I provide a scheme using hexanomial trees (nodes with six branches) which are recombining. This makes the entire scheme highly tractable and accurate.[7] This model achieves the following objectives, contrasting it with existing models:

1. It accommodates a choice of two parameters for varied degrees of skewness and kurtosis.
2. It extends the pricing of interest rate options in the Heath-Jarrow-Morton framework to Poisson-Gaussian processes.
3. The entire lattice used for pricing term structure derivatives can be generated analytically, even in the more complicated Poisson-Gaussian case. This enhances computational *speed.*
4. The scheme used is shown to be recombining, which results in a high degree of computational economy. This feature is found to be retained even when interest rates are mean-reverting. This enables a finer lattice which improves numerical *accuracy.*
5. The discrete-time scheme *converges* to a continuous-time limit.

The model generalizes existing Heath-Jarrow-Morton models in two ways. It generalizes (i) the volatility specification and (ii) adds a jump component without losing the lattice recombination feature. The volatility specification extends the Amin-Morton [5] two parameter form with a four parameter model. The jump specification accounts for both skewness

[7] In discrete-time interest rate models based on trees, when path recombination is not achieved, the number of nodes is of the order of p^n, where p is the number of branches from each node, and n is the number of time steps used in the lattice (tree). In this case, if the number of steps in a binomial ($p = 2$) tree were 30, the number of final nodes would be 2^{30} or approximately 1 trillion nodes. In the recombining hexanomial ($p = 6$) tree here, for 30 time steps, the number of terminal nodes is only 15,376. Of course, for a non- recombining hexanomial tree the number of nodes would be extremely large.

and kurtosis. This fully general form is then taken to gilt market data to demonstrate that both, the Amin-Morton generalized volatility and the jump are incremental features which improve the model fit.

A solution to the Poisson-Gaussian based American-type option pricing problem for stocks was provided by Amin [2]. His model is an extension of the Cox-Ross-Rubinstein [14] approach to pricing stock options. While our paper is analogous in spirit to Amin's work, it represents the solution to a very different problem for the following reasons: (i) Unlike processes used for stocks, interest rate processes assume mean reversion which needs to be accounted for and this complicates the attainment of path-recombination. (ii) With stocks, the drift term does not matter as the mean of the stock price process does not enter the option valuation formula. However, for bonds, the drift terms in the Ito process need to be solved for, such that the prices of bonds in the model match those observed in the market. In this paper, a model of the Poisson-Gaussian process is chosen which permits the computation of the drift terms *analytically*, whereas they often can only be attained numerically. (iii) Most importantly, while spanning is unachievable in equity option models (Merton [29], Amin [2]), and requires asssuming that jump risk is diversifiable or that a price of risk be used, in our model of the term structure spanning is possible, in discrete-time and in the continuous limit.

Our model is the Poisson-Gaussian successor to the pure-Gaussian models of Ho-Lee [25], Heath-Jarrow-Morton [23] and Amin-Bodurtha [6]. These models are of the 'no-arbitrage' family of models, which match the existing term structure of interest rates. Our model uses a discrete-time approach. Convergence of the model to a continuous-time, jump-diffusion limit is demonstrated.

The rest of the paper is as follows: Section Two deals with the theoretical framework for pricing, and Section Three proceeds to provide the computer code and some numerical examples of the implementation of the model. The effects of skewness and kurtosis on bond option prices is analyzed. The model is also applied to gilt bond and option prices and shown to fit better than simple diffusion models. Section Four concludes.

2 The Model

2.1 Discrete-Time Process

Since the model is developed in discrete-time, it is essential to stipulate a discrete time interval, which we denote as h. Whereas it is also possible to index h such that we employ time intervals of varying length, we shall assume without loss of generality that the intervals

are all of equal length. In the model, we will be using risk-neutral pricing methods (a la Harrison & Pliska [22]), and therefore we assume the existence of a probability measure Q, under which the prices of all interest-sensitive assets will follow a martingale.

Assumption 1 Forward Rate Process: *At each trading date t, the forward rates for all future maturities $T > t$ follow the stochastic difference equation:*

$$f(t+h,T) = f(t,T) + \alpha(t,T)h + \sigma(T)X_1(t+h)\sqrt{h} + X_2(t+h)N_{\bar{\lambda},h}, \ \forall T > t \qquad (1)$$

$f(t,T)$ is the one period forward rate at time T, as observed at time t. The drift coefficient of the process is $\alpha(.)$, and the Gaussian coefficient is $\sigma(.)$. We assume that they are bounded. $X_1(.)$ and $X_2(.)$ are random shocks to the process and are assumed to be distributed as follows:

$$\begin{aligned} X_1 &\sim N(0,1) \\ X_2 &= \begin{cases} \mu+\gamma & w/prob \ \frac{1}{2} \\ \mu-\gamma & w/prob \ \frac{1}{2} \end{cases} \end{aligned}$$

X_1 and X_2 are independent random variables. The discrete process above mimics the behavior of a continuous-time jump-diffusion process. Hence, the first noise term above represents the diffusion component, and the second term represents the jump, which takes values $(\mu+\gamma)$ or $(\mu-\gamma)$. Therefore, the jump has mean μ and variance γ^2. $N_{\bar{\lambda},h}$ is an indicator function (representing a point process) taking on the value 1 on rare occasions with probability driven by the parameter $\bar{\lambda}$. $\bar{\lambda}$ is the probability parameter of a jump in unit time, and hence the probability of a jump in any time interval $\approx \bar{\lambda}h$. We assume an infinite number of forward rates in the interval $[0,T]$.

The point process N takes on the value 1 with probability $1 - e^{-\bar{\lambda}h}$. Therefore, we can write the following:

$$N = \begin{cases} 0 & \text{w/prob} \quad 1 - \bar{\lambda}h + o(h) \\ 1 & \text{w/prob} \quad \bar{\lambda}h + o(h) \\ > 1 & \text{w/prob} \quad o(h) \end{cases}$$

For notational convenience, let $\lambda = \bar{\lambda}h$. In the process above, jumps occur rarely, which we achieve by choosing a low value for $\lambda \in (0,1)$, and then we may choose the parameters μ and γ to provide the necessary skewness and kurtosis required. (See the Appendix for the expressions for skewness and kurtosis.) The parameter μ will govern skewness in the model and the parameter γ will drive kurtosis. λ is the jump frequency parameter, which also acts as the mixing parameter providing the composite distribution of (X_1, X_2). Finally, note that the volatility of the diffusion may be different for forward rates of different maturities, i.e., for different T, but the jump component is common across all forward rates. This assumption is made without loss of generality to depict the fact that shocks from jumps affect rates of all maturities.

2.2 Bond Prices

Assuming a continuous compounding convention, we can write out the expressions for the bond price as follows:

$$\begin{aligned} P(t,T) &= \exp\left[-\sum_{i=\frac{t}{h}}^{\frac{T}{h}-1} f(t,ih)h\right] \\ &= \exp\left[-\sum_{i=\frac{t}{h}}^{\frac{T}{h}-1}\left(f(0,ih)+\sum_{j=0}^{i-1}\right.\right. \\ &\quad \left.\left.[\alpha(jh,ih)h+\sigma(ih)X_1((j+1)h)\sqrt{h}+X_2((j+1)h)N((j+1)h)]\right)h\right] \end{aligned} \quad (2)$$

Define the spot rate of interest $r(t)$ as

$$r(t) = f(t,t)$$

Following Harrison & Pliska [22], we define a money market account (numeraire) and assume it is traded. This account is the balance of a reinvested dollar at the spot rate over time.

$$B(t) = \exp\left[\sum_{i=0}^{\frac{t}{h}-1} r(ih)h\right] = \exp\left[\sum_{i=0}^{\frac{t}{h}-1} f(ih,ih)h\right]$$

These definitions will be used later in the model.

2.3 Diffusion (Gaussian Shock) Space

The stochastic term representing the diffusion in equation (1) is $X_1(t)$, and it was assumed to be a standard Normal variate. Therefore, it may be approximated in discrete-time by a binomial tree where the node structure appears as in Figure 1. Thus, the value of X_1 is either +1 or -1 with equal probability. Of course, the entire shock to the forward rate term structure from the Gaussian component is scaled by the appropriate variance term, $\sigma(T), \forall T > t$. The shock $X_1(t)$ applies uniformly to all forward rates, i.e., all rates either move up or down together. This is a natural consequence of the modelling of the diffusion space in this paper as a one-factor model.

2.4 Jump (Poisson Shock) Space

The stochastic term representing the jump in equation (1) is $X_2(t)N(t)$, and it is assumed to be a two-valued random variable activated by a point process. Therefore, if a jump occurs,

it may be represented in discrete-time by a binomial tree where the node structure appears as in Figure 2. It is easily checked that this represents a random variable with mean μ and variance γ^2.

2.5 Poisson-Gaussian Space

The joint effects of the jump and diffusion will be represented by the convolution of the diffusion space and jump space. The diffusion space with the correct noise terms is represented (with attendant probabilities) in Figure 3. The entire jump process $X_2(t)N(t)$ can be represented on a trinomial tree which is as shown in Figure 4, with the necessary probabilities.

The convolution of the two processes provides the outcome for representing the evolution of the entire term structure. This is simply the product space of Figures 3 and 4, which results in a **hexanomial** tree (i.e., each node leads to six other nodes). This is depicted in Figure 5.

2.6 Risk-Neutral Pricing

In discrete-time, it is easy to describe the replication necessary to mimic the payoffs on any contingent claim in this Poisson-Gaussian framework. At all nodes there are six available bonds of different maturities which permit the replication of all possible payoffs under the six outcomes in the state space in the next period. Given an entire available term structure of bonds, this is easily achieved. A similar complete markets replication argument was first employed by Jarrow and Madan [26] in a recent paper on the use of the term structure to hedge jumps in the pricing of derivatives on risky assets.

Since the payoffs are replicable, the state space is spanned. This means that, as delineated in Harrison and Pliska [22]. there exists a risk-neutral probability measure Q, under which the prices of all interest-sensitive securities follow a martingale. It is also well-known (see Harrison and Kreps [21]) that the existence of this martingale measure is equivalent to the existence of no-arbitrage, and therefore the prices we will compute will be arbitrage free.

An exact set of six bonds can be used to span the uncertainty at each node, and thus a unique replication is also achieved. The unique spanning of the state space ensures that markets are complete. Therefore, completeness of markets ensures a unique martingale measure for the pricing of securities. Utilizing this specification allows us to compute the drift terms $\alpha(t,T)$ consistent with the martingale condition. Define the process for discounted

bonds as follows, using the numeraire $B(t)$:

$$Z(t,T) = \frac{P(t,T)}{B(t)}$$

In the absence of arbitrage, the prices of discounted assets follows a martingale under the measure Q, i.e.,

$$E_t^Q\left[\frac{Z(t+h,T)}{Z(t,T)}\right] = 1$$

Proceeding as in Amin & Bodurtha [6], we can write

$$\frac{B(t+h)}{B(t)} = \exp[r(t)h] = \exp[f(t,t)h]$$

and

$$\frac{P(t+h,T)}{P(t,T)} = \frac{\exp[-\sum_{j=\frac{t}{h}+1}^{\frac{T}{h}-1} f(t+h,jh)h]}{\exp[-\sum_{j=\frac{t}{h}}^{\frac{T}{h}-1} f(t,jh)h]}$$

$$= \exp[f(t,t)h - \sum_{j=\frac{t}{h}+1}^{\frac{T}{h}-1} (f(t+h,jh) - f(t,jh))h]$$

Combining the equations above, we arrive at the following expression:

$$\frac{Z(t+h,T)}{Z(t,T)}$$
$$= \exp\left[-\sum_{j=\frac{t}{h}+1}^{\frac{T}{h}-1} [\alpha(t.jh)h + \sigma(jh)X_1((j+1)h)\sqrt{h} + \frac{1}{h}(T-t)X_2((j+1)h)N((j+1)h)]h\right]$$

Taking expectations under the risk-neutral measure on both sides and equating to 1 (i.e., using the martingale condition, $E_t^Q[\frac{Z(t+h,T)}{Z(t,T)}] = 1$) results in the following Lemma:

Lemma 1 Risk-Neutral Drifts *The following expression for the drift $\alpha(t,.)$ ensures that the prices of interest rate securities follows a martingale:*

$$\left[\sum_{j=\frac{t}{h}+1}^{\frac{T}{h}} \alpha(t.jh)h\right] h$$
$$= \log\left[E_t^Q \exp\left(\left[\sum_{j=\frac{t}{h}+1}^{\frac{T}{h}} \sigma(jh)X_1(t+h)\sqrt{h} + \frac{1}{h}(T-t)X_2(t+h)N(t+h)\right] h\right)\right] \quad (3)$$

When expanded out, the above expression appears as follows:

$$\left[\sum_{j=\frac{t}{h}+1}^{\frac{T}{h}} \alpha(t,jh)h\right] h = \log(A)$$

where

$$\begin{aligned}
A \;=\; & \exp\left(\left[-\sum_{j=\frac{t}{h}+1}^{\frac{T}{h}} \sigma(jh)\sqrt{h} + \frac{1}{h}(T-t)(-\mu-\gamma)\right] h\right) \times \frac{\lambda}{4} \\
& + \exp\left(\left[-\sum_{j=\frac{t}{h}+1}^{\frac{T}{h}} \sigma(jh)\sqrt{h}\right] h\right) \times \frac{1-\lambda}{2} \\
& + \exp\left(\left[-\sum_{j=\frac{t}{h}+1}^{\frac{T}{h}} \sigma(jh)\sqrt{h} + \frac{1}{h}(T-t)(-\mu+\gamma)\right] h\right) \times \frac{\lambda}{4} \\
& + \exp\left(\left[\sum_{j=\frac{t}{h}+1}^{\frac{T}{h}} \sigma(jh)\sqrt{h} + \frac{1}{h}(T-t)(-\mu-\gamma)\right] h\right) \times \frac{\lambda}{4} \\
& + \exp\left(\left[\sum_{j=\frac{t}{h}+1}^{\frac{T}{h}} \sigma(jh)\sqrt{h}\right] h\right) \times \frac{1-\lambda}{2} \\
& + \exp\left(\left[\sum_{j=\frac{t}{h}+1}^{\frac{T}{h}} \sigma(jh)\sqrt{h} + \frac{1}{h}(T-t)(-\mu+\gamma)\right] h\right) \times \frac{\lambda}{4}
\end{aligned}$$

This equation for the drift can be elucidated with a perusal of Figure 5. Since we can represent the evolution of the process using a hexanomial tree, the drift term contains six terms as is shown above. Once the drifts have been solved for, it is easy to draw the risk-neutral hexanomial tree for the evolution of the term structure of forward rates. Note that here the drifts are computed analytically, making the computer implementation of the model fast and efficient.

2.7 Tree Recombination and Tree Size

Since none of the terms in the analytical expression for the drifts is a function of the state variable $f(t.T), \forall t < T$, the drifts, which are additive across time, are not a function of the nodal position on the tree. This makes the tree recombining.

Recombination is a valuable property for a numerical scheme of this sort as it enables numerical tractability, since computations are kept at an economical number. In the absence

of recombination, each node on the hexanomial tree would branch out into six new nodes, and this would lead to a tree that would rapidly prove to be numerically unmanageable. With recombination, it is easy to demonstrate that this problem does not arise, and in the following paragraphs we shall actually compute exactly the number of nodes based on the number of time steps established on the tree. Increasing the number of time steps economically (because of recombination) enhances the convergence and accuracy of the numerical scheme employed.

Understanding the features of the hexanomial tree is essential to its numerical implementation, as well as being required to assess the number of nodes. To do so, we refer to Figure 6, which depicts the diffusion space drawn out two periods. It is quite clear that the number of nodes in diffusion space grows exactly as the number of time periods on the lattice. After one period, there are two nodes, and after two periods there are three nodes. Therefore,

$$\text{No. of nodes in diffusion space after } n \text{ periods} = n + 1$$

A similar diagram is drawn for the jump space, and presents a different type of series. Turning to Figure 7, we see the evolution of the tree in jump space. Here we can see that the first node leads to three new nodes. However, after two periods, instead of nine nodes, we obtain only six. In fact, the number of nodes grows as per the following formula:

$$\text{No. of nodes in jump space after } n \text{ periods} = \frac{1}{2}(n+1)(n+2)$$

As we have already seen, the risk neutral drifts are not functions of the forward rates, thus enabling a recombining lattice. Since this tree is necessarily recombining, it is therefore formed by the product space made up of the diffusion and jump spaces. Analogously, the number of nodes will also be the product of the number of nodes in diffusion and jump space, i.e.,

$$\text{No. of nodes in Poisson-Gaussian space after } n \text{ periods} = \frac{1}{2}(n+1)^2(n+2)$$

Table 2 provides the number of nodes for several values of n. It is easy to see that even with a large number of time steps, the number of nodes does not grow too large. Thus the economical number of nodes allows more time steps and therefore accurate evaluation of interest rate derivative securities when the term structure follows a Poisson-Gaussian process.

2.8 Mean Reversion & Path-Recombination

As shown in Heath-Jarrow-Morton [23], the appropriate choice of the volatility function $\sigma(T), \forall t < T$ allows a tree to be established which is consistent with a mean-reverting process for the spot rate. In particular, the following choice of the volatility specification enables mean reversion and yet retains the feature of path-recombination:

$$\sigma(T) = \sigma \exp[\beta(T)]$$

where the coefficient of mean reversion $\beta(T)$ is decreasing in T. A simple specification that is often used is

$$\sigma(T) = \sigma \exp[-\beta(T)], \ \forall T > t$$

Since this specification does not contain the state variable, i.e., the forward rates, it retains the feature of path-recombination. The analytic expression for the risk-neutral drifts in equation (3) is modified to contain the exact form of the volatility function chosen. While this feature was routinely employed in pure-Gaussian models (see HJM [23]), it has now been extended to the realm of Poisson-Gaussian models.

One criticism of some generalized volatility models, and the generalized Vasicek model in this paper is that interest rates can become negative. The model approach in this paper may be extended to include proportional models. Of course, the injection of the mean reversion feature reduces the possibility of negative rates on the lattice.

2.9 Convergence to the Continuous-Time Limit

In this section, we shall derive the continuous-time form of the discrete-time stochastic difference equation (1). Let D be the metric space of RCLL (right continuous functions with left limits) real-valued functions on $[0,T]$. Let the sequence of forward rate processes be defined on the path space $D[0,T]$. Let $C[0,T]$ be the subspace of $D[0,T]$ of all real-valued continuous functions on $[0,T]$. The space D is restricted to the Skorokhod topology, which when restricted to the space $C[0,T]$ is the topology of uniform convergence.

First, we prove that the discrete point process $N_{\bar{\lambda},h}$ converges to a Poission process. Consider the time interval h. Let the random variable q denote the number of jumps in the interval. Divide h into n intervals of length m each, i.e., $m = \frac{h}{n}$. Let y_j be the number of jumps in subinterval j. Then $q = \sum_{j=1}^{n} y_j$ and the following probability set up is true in each subinterval:

$$\begin{aligned} \text{Prob}(y_j = 0) &= 1 - \bar{\lambda}m + O(m) \\ \text{Prob}(y_j = 1) &= \bar{\lambda}m + O(m), \ \forall j \end{aligned}$$

Therefore, for large n, y_j follows a Bernoulli distribution as the probability of $y_j > 1 \approx O(m)$. This Bernoulli distribution has parameter $\bar{\lambda}m = \bar{\lambda}h/n$. Then q, which is the sum of Bernoulli random variables, must be distributed Binomial, such that

$$\text{Prob}(q = l) \approx \binom{n}{l} \left(\frac{\bar{\lambda}h}{n}\right)^{l} \left(1 - \frac{\bar{\lambda}h}{n}\right)^{n-l}, \ l = 0, 1, 2...n$$

Taking the limit, the process q has the density:

$$\lim_{n\to\infty}\binom{n}{l}\left(\frac{\bar{\lambda}h}{n}\right)^{l}\left(1-\frac{\bar{\lambda}h}{n}\right)^{n-l}=\frac{(e^{-\bar{\lambda}}h)(\bar{\lambda}h)^{l}}{l!}$$

which is clearly Poisson in the limit. Therefore the process $N_{\bar{\lambda},h}$ converges to a Poisson process. Let us denote this limiting process as $G(t)$.

Rewriting equation (1), we obtain

$$f(t,T)=f(0,T)+\sum_{j=0}^{\frac{t}{h}-1}\alpha(jh,T)h+\sum_{j=0}^{\frac{t}{h}-1}\sigma(T)X_1(jh)\sqrt{h}+\sum_{j=0}^{\frac{t}{h}-1}X_2(jh)N(jh)$$

Taking limits ($h\downarrow 0$), and applying Donsker's Theorem (Duffie, [18], pg 248) to the diffusion part and recognizing that the jump component is simply a compound Poisson process (see Karlin & Taylor, [27], pg 426), we obtain

$$f(t,T)=f(0,T)+\int_0^t\alpha(s,T)\,ds+\int_0^t\sigma(T)\,dW_1(s)+\int_0^t J(\mu,\gamma^2)(s)\,dG(s) \tag{4}$$

where $W_1(t)$ is a standard Brownian Motion, and $J(\mu,\gamma^2)$ is a two-state random variable with mean μ and variance γ^2. Finally, taking the differential provides the stochastic differential equation

$$df(t,T)=\alpha(t,T)\,dt+\sigma(T)\,dW_1(t)+J(t)\,dG(t) \tag{5}$$

which is the continuous-time limit of the stochastic difference equation (1).

While it is clear that spanning, and hence market completeness is easily achieved in the discrete hexanomial model, we need to be sure that it is also obtained in the continuous-time limit. This is certainly the case, as a wide spectrum of bonds is available on the term structure, and similar arguments to that of Jarrow and Madan [26] apply, i.e. a finite risk space may be spanned using the term structure. In the model in this paper, in continuous-time, spanning is implementable with a finite set of securities (bonds). To see this, note that we can write equation (5) in an alternate fashion as follows:

$$df(t,T)=\alpha(t,T)\,dt+\sigma(T)\,dW_1(t)+J_1(t)\,dG_1(t)+J_2(t)\,dG_2(t),\ \ \forall T\geq t$$

with the Poisson frequency parameter for processes G_1 and G_2 being $\frac{\lambda}{2}$ each, and the jumps being of constant size such that $J_1(t)=\mu+\gamma, J_2(t)=\mu-\gamma, \forall t$ (proof in Appendix). Following from the boundedness of $\alpha(.)$ and $\sigma(.)$ in Assumption 1, we assume that

$$\int_0^T\mid\alpha(t,T)\mid\,dt<+\infty\ \ a.e.Q$$

$$\int_0^T\sigma^2(T)\,dt<+\infty\ \ a.e.Q$$

which are the usual integrability conditions.

Our bond prices are simply the exponential integral over the forward rates: $P(t,T) = \exp[-\int_t^T f(t,s)\,ds]$. Using an extension of Heath-Jarrow-Morton [23] pg 82, it can be shown that with jump-diffusions, the bond price process is as follows:

$$\begin{aligned}
\frac{dP(t,T)}{P(t,T)} &= [a(t,T) + \frac{1}{2}b(t,T)^2]\,dt + b(t,T)\,dW_1(t) \\
&\quad + [e^{-J_1(T-t)} - 1]\,dG_1(t) + [e^{-J_2(T-t)} - 1]\,dG_2(t) \\
a(t,T) &= -\int_t^T \alpha(t,v)\,dv \\
b(t,T) &= -\int_t^T \sigma(v)\,dv
\end{aligned} \tag{6}$$

A proof of this result follows in the Appendix. For each T, and fixing t, we can write equation (6) in a more economical form as follows:

$$\frac{dP(T)}{P(T)} = M(T)\,dt + V(T)\,dW_1 + H_1(T)\,dG_1 + H_2(T)\,dG_2$$

This follows from equation (6) since for a given T, the coefficients are deterministic constants. By splitting the initial Poisson process with a random jump into two Poisson processes with constant jumps, we achieve a process with three sources of noise, a diffusion element and two jump elements.

In order to price derivative securities, we need to show spanning and market completeness. Spanning arguments in the case of jump-diffusion processes have been developed by both Shirakawa [34] and Jarrow and Madan [26], and they are outlined in brief here. Assume that there are three available bonds on the term structure, with maturities T_1, T_2, T_3 such that the risk matrix

$$\begin{bmatrix} V(T_1) & H_1(T_1) & H_2(T_1) \\ V(T_2) & H_1(T_2) & H_2(T_2) \\ V(T_3) & H_1(T_3) & H_2(T_3) \end{bmatrix} \tag{7}$$

is non-singular. Given this the matrix is invertible and we are able to span the state space with our three securities. Following theorem 2.1 of Shirakawa [34], we then assume that there are no arbitrage opportunities in the market. This implies that the expected drift functions for the forward rate processes take the following form:

$$M(T) = b(t,T)\phi - \sum_{i=1}^{2}[e^{-J_i(T-t)} - 1]\psi_i$$

where ϕ, ψ_1, ψ_2 are risk premiums for the three sources of risk in the model. Given the

non-singularity of (7), we can express these risk premiums as follows:

$$\begin{pmatrix} \phi(t) \\ \psi_1(t) \\ \psi_2(t) \end{pmatrix} = \begin{bmatrix} V(T_1) & H_1(T_1) & H_2(T_1) \\ V(T_2) & H_1(T_2) & H_2(T_2) \\ V(T_3) & H_1(T_3) & H_2(T_3) \end{bmatrix}^{-1} \begin{pmatrix} M(T_1) - \sum_{i=1}^{2} H_i(T_1)\frac{\lambda}{2} \\ M(T_2) - \sum_{i=1}^{2} H_i(T_2)\frac{\lambda}{2} \\ M(T_3) - \sum_{i=1}^{2} H_i(T_3)\frac{\lambda}{2} \end{pmatrix}$$

Since the RHS of the equation must hold for any t, the LHS is independent of t, and can be written as $[\phi, \psi_1, \psi_2]'$. Further, in addition to spanning, the existence an equivalent martingale measure and unique risk-premia imply market-completeness (see Shirakawa, theorem 2.2). This allows the creation of a replicating self-financing strategy to mimic the value of an American option. Arbitrage-free pricing is thus achieved in the continuous-time limit. Unlike pricing with jumps for equities, where spanning is not achievable, the term structure application permits spanning. Thus, we do not require to resort to assumptions that jump risk is unsystematic (Merton [29]) nor to a version of the model where incompleteness is priced (Amin [2]).

Since we have shown that the discrete process converges weakly in D to the continuous process in equation (5), and that simple assumptions assure that spanning is attained, we know that in continuous-time arbitrage free pricing is possible. The definition of weak convergence assures us that the prices of European options will converge to their continuous-time limits under mild regularity conditions, such as assuming that the option payoffs are continuous and uniformly integrable (see Duffie [19], pgs 198-199). For American-type options, we also need to show that the sequence of value functions obtained from the optimal stopping problem in discrete-time converges to a continuous-time limit. Once again, Amin and Khanna [4] have shown that in general, by assuming simple uniform integrability conditions, the convergence to the limit is assured, and in particular, if spanning is achieved (i.e. complete markets), one can replicate the American option by trading in the underlying securities (see Amin and Jarrow [3]). In a similar vein, Kushner and DiMasi [28] show that in a jump-diffusion optimal control problem, convergence is attained with boundedness conditions on the coefficients of the underlying process, which are also met. Therefore, assuming bounded coefficients, that the option payoff is continuous, and is uniformly integrable, application of the continuous mapping theorem (Duffie [19] pg 199) provides convergence of derivative security prices to continuous-time limits.

3 Numerical Implementation of the Model

Whereas the theoretical development of the model has been carried out within a simple diagrammatic framework, and most of the working pieces of the model have been analytically derived, in such models the computer implementation can potentially prove to be complex.

In fact, compared to lattice methods which fit the smile, the computer program is extremely economical. This feature follows directly from the simple theoretical approach employed. Two modelling features are particularly useful: (i) the fact that the drift terms are analytically expressed (equation 3) eliminates the need for costly code to solve for the drifts numerically; (ii) the path-recombination feature of the scheme used which ensures a parsimonious implementation. Usually, 'fitting the smile' methods require the solution of systems of equations while setting up the lattice. Our tree, despite its hexanomial form, requires no such computations. In fact, the computer code for the model is extremely economical, given the closed-form derivation of the model drift terms (see the Appendix for the program code).

3.1 Examples

In this section, we shall compare option values from a Poisson-Gaussian model versus those from a pure-Gaussian model, in environments where we allow skewness and kurtosis to vary. This is simple to implement as in order to obtain a pure-Gaussian model from our Poisson-Gaussian program, all we need to do is to set the parameter for jump arrival, λ, to zero.

In order to illustrate the operation of the model, I have priced options for varying skewness and kurtosis coefficients, and Figures 8-12 depict option prices. In Figure 8, we price a 2.5-year European option on a 5-year default free \$100 zero coupon bond. The exercise price of the option is computed to be the at-the-money forward price of the bond 2.5 years forward. The plot provides call option prices for three choices of skewness: positive skewness ($\mu = 0.005$)(50 basis points), zero skewness ($\mu = 0$) and negative skewness ($\mu = -0.005$). For each skewness level, we plot the value of the option for a range of short interest rates from 5% to 15%. The exercise prices are also adjusted so as to remain at-the-money forward. (In Figures 9 and 10, we shall explore the effects of skewness when the exercise price is held constant.) The option values are higher when interest rates are skewed, either positively or negatively. Option values are lower when interest rates display no skewness. While this may appear counterintuitive, it is easily explained. When skewness is positive, interest rates move upwards and this reduces bond prices, but the present value of the exercise price declines, adding value to the option. The trade-off between the time value and intrinsic value is such that while intrinsic value falls, time value more than compensates for this effect and the overall value of the option increases. Since the option is at-the-money forward, intrinsic value falls to a floor of zero, and time value has an unlimited upside, adding a net positive effect to the value of the option. When skewness is negative, interest rates move down and the intrinsic value of the call option moves up; on the other hand, the time value reduces but now the net effect is positive as well, since intrinsic value is no longer capped and its effect outweighs that of time value. Therefore skewness appears to have a symmetric effect on the pricing of bond options, struck at-the-money forward. This is in contrast to the effects

noticed in the pricing of stock options where skewness clearly operates asymmetrically.

The analysis in Figure 8 dealt with options that were purely at-the-money forward. [8] In Figures 9 and 10, we analyze the effects of skewness for options that are priced at varying degrees of moneyness. This is done by keeping the exercise price fixed at the at-the-money forward price corresponding to a short rate level of 10%. In Figure 9, a plot of the difference in call option prices between the skewness models and zero skewness models is shown. There are two plots: one for the difference in option value between the negative skewness model and zero skewness model, and one for the difference between the positive skewness model and the zero skewness model. Interest rates are varied from 5% to 15%. In Figure 9, the plots relate to a 3-year option on a 6-year zero coupon bond. As can be seen, with positively skewed interest rates, the in-the-money options tend to be priced higher (time value effects dominate the intrinsic value effects), and with negative skewness, the out-of-the-money options are priced higher (intrinsic value effects dominate the time value effects) relative to the the zero skewness case. In Figure 10, a similar exercise is undertaken for the 5-year option on a 10-year zero-coupon bond. Results are similar.

To illustrate the effect of kurtosis, option pricing results are portrayed in Figures 11 and 12. In Figure 11, we plot the difference between the prices of bond options priced using the Poisson-Gaussian model, and prices from a pure-Gaussian model in which the diffusion volatility is adjusted upwards in order to ensure the same level of total volatility per unit time as the Poisson-Gaussian model. The plot is made for three different choices of the standard deviation of the jump: 10, 60 and 100 basis points. Skewness is set to zero. Prices are presented for a 3-year European call option on a 6-year \$100 zero coupon bond. The exercise price is the at-the-money forward price for a 10% short rate, which is \$72.33. The interest rate is varied from 5% to 15%. Thus we obtain a range of option prices varying from deep in-the-money to deep out-of-the-money values. As is to be expected, when the variance of the jump is very low (10 basis points), there is little difference between the Poisson-Gaussian and pure-Gaussian models. However, as the variance of the jump effect rises, at-the-money option values from the Poisson-Gaussian model drop below those from a pure-Gaussian model. The opposite effect is noticed for out-of-the-money and in-the-money options which are priced higher relative to the pure-Gaussian model. This is because when interest rates follow a Poisson-Gaussian process, the distribution of interest rates becomes fat-tailed, and peaked around the mean. The greater the jump variance, the more marked

[8] Reasonable parameter values are used. For example the short rate r_0 is varied from 5% to 15%. The functional form used for the forward rate term structure is a simple one, rising steeply at first and then flattening out, which is quite often observed ($f(t) = r_0 + \ln(t)/200$). Skewness (μ) is varied from +100 to -100 basis points. Kurtosis (γ) is assumed to be about 100 basis points. Volatility decay is at the rate of $\beta = 0.1$ which translates into a mean reversion rate of the same magnitude. And finally the jump frequency is taken to be $\lambda = 0.1$ which provides a 10% probability of a jump per time period.

this effect. In Figure 12, an identical exercise is undertaken for the 5-year option on the 10-year bond, and a similar effect is noticed. These results in the case of bond options are very similar to those evidenced in the case of equity options. These effects were first documented by Merton, who arrived at similar figures in an early paper [30].

3.2 A Brief Empirical Examination

In this section, we report the performance of the model on options in the U.K. bond markets. The term structure of U.K. gilt interest rates and cap options with maturities out to 10 years are used to fit the model and compare it to a model which does not employ the jump feature.

The model has been fit using a genetic algorithm which minimizes the percentage error in prices. Data for 3 days, 1-Feb-95 to 3-Feb-95, is used to calibrate the model. The yield curve each day goes out to a maturity of 11 years, and the tree is drawn with a timestep of 0.25 years. Market prices for caps go out to 10 years, and have individual caplets every half year.

The first model that was fitted was one with constant volatility (σ) for the diffusion process. This provides a simple model which is analogous to enhancing the Ho-Lee model [25] with the jump process in this paper. Thus the numerical procedure fits the prices of bonds and caps on this tree by finding the optimal values of the parameters $[\sigma, \lambda, \mu, \gamma]$. Of course, the drift terms are computed during the implementation on the tree as well.

Table 3 presents the results of the fitting procedure. For each of the three days examined, the table reports parameter values, and the average percentage pricing error. The value of σ is reported in basis points per annum, and μ, γ are reported in basis points. With the constant volatility model the parameter estimates are quite unstable from day to day. Also notice that the size of the jump given by the parameter γ is quite small. This implementation of the model, with constant volatility, behaves more like a mixture of distributions than a jump-diffusion model, as the probability of a jump is often close to fifty percent. There is positive skewness injected by the jump feature, i.e. parameter μ. However, the model does not fit very well, since for long maturities, it is well known that constant volatility models do not do very well. The additional jump feature does little to capture long dated effects. In fact, the effect of jumps is more likely to provide a better fit for short dated options which are affected by kurtosis.

The poor fit of the model can be ascribed to the fact that the volatility term structure is not flat. In fact, it is humped, which is a usual occurence in the markets. Table 4 reports the raw term structure of volatilities rounded to 25 basis points extracted from fitting the cap prices to a simple Black [8] model which assumes a lognormal process for zero coupon

forward bond prices. It is apparent that the term structure of volatility rises and then falls. The model will not fit this well with a constant volatility parameter. Therefore, the use of generalized volatility models such as those chosen in Amin and Morton [5] is posited. However, the 2 parameter models used there do not provide for a humped term structure of volatilities. Instead. here we develop a more generalized model which is a four parameter form, as follows:

$$\sigma(T) = A + B\exp(-T/D) + C\frac{T}{D}\exp(-T/D)$$

which requires parameters $[A, B, C, D]$. This model captures the level, slope and curvature of the term structure of volatilities. Parameter A governs the level of the term structure, parameter B controls the slope, and finally, parameter C controls the curvature. The last parameter D, is a damping or fitting parameter. For each T, the volatility of forward rates is provided by the model above, giving a complete term structure of volatilities.

Table 5 reports the fit of the Poisson Gaussian model with the generalized volatility structure. The model now possesses 7 parameters: $[A, B, C, D, \lambda, \mu, \gamma]$. The fit improves drastically with the new volatility model. The percentage pricing error is reduced by about 5 times. Once again positive skewness is evidenced, and kurtosis varies a lot from day to day. However, the jump feature is now seen to be a rarer event, with the probability of a jump ranging from approximately 5% to 10%. Therefore, jumps are now parametrically rare events. This suggests that the simple addition of a volatility term structure is essential in capturing the prices of options.

In order to examine the effect of the jump feature, the generalized volatility model was calibrated without the jump feature. The results are presented in Table 6. The model does not fit as well as the full generalized volatility jump diffusion model. Hence, clearly the additional jump parameters do capture the prices of options better. The presence of skewness and kurtosis in the data suggests the use of the additional jump feature.

4 Conclusion

This paper extends the literature on the pricing of American-type bond options for pure-Gaussian processes to Poisson-Gaussian processes. The effects of skewness and kurtosis in the HJM model have been injected before with stochastic volatility models. This paper provides for this feature by adding a jump component, in addition to generalized volatility. We provide a simple. tractable, accurate and convergent Poisson-Gaussian model for the pricing of interest rate derivatives, which provides the user a means to inject the necessary amount of skewness and kurtosis desired into pricing models. Numerical examples illustrate the implementation of the model, and provide intuition regarding the effects of skewness

and kurtosis on the term structure on the values of option prices. In summary, the paper generalizes the Amin-Morton [5] class of models by adding (i) a more flexible volatility specification, and (ii) a jump component, yet retaining the lattice recombination feature, which is extremely useful for practical applications.

The Poisson-Gaussian process is specified using a hexanomial tree (six nodes emanating from each node), and the tree is shown to be recombining. This feature of the tree ensures path-recombination. A fairly general class of volatilities preserving path-recombination and providing mean reversion is attainable even under this enhanced Poisson-Gaussian framework. The features of the model are examined with numerical simulations, and the model is also taken to gilt market data. It is seen that the introduction of generalized volatility and jumps plays a key role in better fitting options prices.

References

[1] Ait-Sahalia. Y, "Testing Continuous-Time Models of the Interest Rate," 1995, forthcoming *Review of Financial Studies.*

[2] Amin, K, "Jump-Diffusion Option Valuation in Discrete Time," *Journal of Finance*, 1993, v48(5). 1833-1863.

[3] Amin, K., and R. Jarrow, "Pricing Options on Risky Assets in a Stochastic Interest Rate Economy," *Mathematical Finance*, 1992, v2(4), 217-237.

[4] Amin, K., and A. Khanna, "Convergence of American Option Values from Discrete to Continuous-Time Financial Models," *Mathematical Finance*, 1993,

[5] Amin, K., and A. Morton, "Implied Volatility Functions in Heath-Jarrow-Morton Models," *Journal of Financial Economics*, 1994. ...

[6] Amin, K., and J. Bodurtha, "Discrete-Time Valuation of American Options with Stochastic Interest Rates," *Review of Financial Studies*, 1995, v8(1), 193-234.

[7] Ahn, Chang Mo and Howard E. Thompson, "Jump-Diffusion Processes And Term Structure Of Interest Rates," *Journal of Finance*, 1988, v43(1), 155-174.

[8] Black, Fischer.. "The Pricing of Commodity Contracts," *Journal of Financial Economics*. 1976, v2(1). 167-179.

[9] Brennan, M. & E. Schwartz, "A continuous-time Approach to the Pricing of Bonds," *Journal of Banking & Finance*, 1979, 133-155.

[10] Brenner, R.. R. Harjes, and K. Kroner, "Another Look at Alternative Models of the Short-Term Interest Rate," 1994, unpublished manuscript, Merrill Lynch, Wells Fargo and University of Arizona.

[11] Carverhill, Andrew. "A Simplified Exposition of the Heath, Jarrow and Morton Model," *Stochastics and Stochastics Reports*, 1995, v53, 227-240.

[12] Chan, K.C.. G.A. Karolyi, F.A. Longstaff, and A.B. Sanders, "An Empirical Comparison of Alternative Models of the Short-Term Interest Rate," *Journal of Finance*, 1992, v47(3). 1209-1228.

[13] Cox, John C., Jon E. Ingersoll, and Stephen A. Ross, "A Theory of the Term Structure of Interest Rates." *Econometrica*, 1985b, 385-407.

[14] Cox, J.. S. Ross., and M. Rubinstein, "Option Pricing: A Simplified Approach," *Journal of Financial Economics*, 1979, v7, 229-263.

[15] Das, Sanjiv, "Poisson-Gaussian Processes and the Bond Markets," 1994, Harvard Business School, Working Paper.

[16] Das, Sanjiv, "Discrete-Time Bond and Option Pricing for Jump-Diffusion Processes," 1994, Harvard Business School, Working Paper.

[17] Derman, Emanuel., and Iraj Kani, "Riding on a Smile," *Risk*, 1994, February, v7(2), 32-38.

[18] Duffie, D, "Security Markets - Stochastic Models," 1988, Academic Press, California.

[19] Duffie, D, "Dynamic Asset Pricing Theory," 1992, Princeton University Press, New Jersey.

[20] Dupire. Bruno, "Pricing with a Smile," *Risk*, 1994, January, v7(1), 18-20.

[21] Harrison, J.M., and D. Kreps, "Martingales and Arbitrage in Multiperiod Securities Markets," *Journal of Economic Theory*, 1979, v20, 381-408.

[22] Harrison, J.M., and S. Pliska, "Martingales and Stochastic Integrals in the Theory of Continuous Trading." *Stochastic Processes and their Applications*, 1981, v11, 215-260.

[23] Heath, D., R. Jarrow, & A. Morton, "Bond Pricing and the Term Structure of Interest Rates: A Discrete-Time Approximation," *Journal of Financial and Quantitative Analysis*, 1990, v25. 419-440.

[24] Heston. S, "A Model of Discontinuous Interest Rate Behavior, Yield Curves and Volatility," 1995, Working Paper, Washington University, St. Louis.

[25] Ho, T. & S. Lee, "Term Structure Movements and Pricing Interest Rate Contingent Claims." *Journal of Finance*, 1986, v41, 1011-1029.

[26] Jarrow. R., and D. Madan, "Option Pricing using the Term Structure of Interest Rates to Hedge Systematic Discontinuities in Asset Returns," 1995, forthcoming *Mathematical Finance*.

[27] Karlin, S., and H.M. Taylor, "A Second Course in Stochastic Processes," 1981, Academic Press, California.

[28] Kushner, H., and G. DiMasi, "Approximations for Functionals and Optimal Control on Jump-diffusion Processes," *Journal of Mathematical Analysis and Applications*, 1978, v40, 772-800.

[29] Merton. R.C.. "Option Pricing when underlying Stock Returns are Discontinuous," *Journal of Financial Economics*, 1976. v3, 125-144.

[30] Merton. Robert, C., "The Impact on Option Pricing of Specification Error in the Underlying Stock Price Returns," *Journal of Finance*, 1976, v31(2), 333-351.

[31] Naik, V. and Moon H. Lee. "The Yield Curve and Bond Option Prices with Discrete Shifts in Economic Regimes," Working Paper, University of British Columbia, 1993.

[32] Ritchken, Peter., and L. Sankarasubramanian, "Volatility Structures of Forward Rates and the Dynamics of the Term Structure," Mathematical Finance, 1995, January, v5(1), 55-72.

[33] Rubinstein, Mark, "Implied Binomial Trees," *Journal of Finance*, 1994, July, v49(3), 771-818.

[34] Shirakawa, H, "Interest Rate Option Pricing with Poisson-Gaussian Forward Rate Curves," *Mathematical Finance*, 1991. v1(4), 77-94.

[35] Vasicek, O, "An Equilibrium Characterization of the Term Structure," *Journal of Financial Economics*, 1977, v5, 177-188.

A Proofs

A.1 *Moments of the Discrete Process*

The moments of the discrete process provide the intuition for why the choice of jump form injects the necessary skewness and kurtosis into the model. The first four moments are as follows:

1. Mean:
$$E[f(t+h,T)] = f(t,T) + \alpha(t,T) + \lambda\mu$$

2. Variance:
$$V[f(t+h,T)] = \lambda(\mu^2+\gamma^2) - \lambda^2\mu^2 + h\sigma^2$$

3. Skewness:
$$Sk[f(t+h,T)] = (1-\lambda)\lambda\mu(3\gamma^2+\mu^2-2\lambda\mu^2)$$
the sign of which clearly depends on the sign of μ.

4. Kurtosis: This is expressed for $\sigma = 0$ and $\mu = 0$, to keep the expression simple and to observe the effect of γ.
$$Ku[f(t+h,t)] = \lambda\gamma^4$$
which demonstrates that the magnitude of kurtosis depends on the size of γ. When $\mu \neq 0$. kurtosis is equal to $(1-\lambda)\lambda^4\mu^4 + \frac{\lambda}{2}(\mu-\gamma-\lambda\mu)^4 + \frac{\lambda}{2}(\mu+\gamma-\lambda\mu)^4$, which means the sign and size of μ also affects the degree of kurtosis. However, here too, the degree of kurtosis increases with γ.

A.2 *Splitting the Jump Process*

We need to show that $J\,dG(\lambda) = J_1\,dG_1(\frac{\lambda}{2}) + J_2\,dG_2(\frac{\lambda}{2})$. where

$$J = \begin{cases} \mu+\gamma & \text{w/prob } \frac{1}{2} \\ \mu-\gamma & \text{w/prob } \frac{1}{2} \end{cases}$$

We can also see that

$$J\,dG = \begin{cases} \mu+\gamma & \text{w/prob } \frac{\lambda\,dt}{2} \\ 0 & \text{w/prob } 1-\lambda\,dt \\ \mu-\gamma & \text{w/prob } \frac{\lambda\,dt}{2} \end{cases} \tag{8}$$

Now dealing with $J_1\,dG_1 + J_2\,dG_2$, we can work out the probabilities as follows. The probability of both dG_1 and dG_2 occuring is $\frac{\lambda\,dt}{2} \times \frac{\lambda\,dt}{2} = 0$, because $dt^2 = 0$. The probability

that dG_1 occurs but dG_2 does not is $\frac{\lambda\,dt}{2} \times (1 - \frac{\lambda\,dt}{2}) = \frac{\lambda\,dt}{2}$, and the value of the jump is $\mu + \gamma$. The probability that dG_2 occurs but dG_1 does not is $(1 - \frac{\lambda\,dt}{2}) \times \frac{\lambda\,dt}{2} = \frac{\lambda\,dt}{2}$, and the value of the jump is $\mu - \gamma$. The probability that both dG_1 and dG_2 do not occur not is $(1 - \frac{\lambda\,dt}{2}) \times (1 - \frac{\lambda\,dt}{2}) = 1 - \lambda\,dt$, and the value of the jump is 0. Notice that this gives the same values and probabilities as in (8) and so the two jump forms are equivalent. This is a useful means of transforming a Poisson process with a finite state-space random jump size into a set of constant jump Poisson processes.

A.3 *Heuristic Derivation of the dP process*

Taking a simple case (one period)

$$df = \alpha\,dt + \sigma\,dw + J_1\,dG_1 + J_2\,dG_2$$

and

$$P(f) = e^{-f}$$

Then, using the jump-diffusion version of Ito's Lemma,

$$dP = -P(\alpha\,dt + \sigma\,dw) + \frac{1}{2}\sigma^2 P\,dt + P[e^{-J_1} - 1]\,dG_1 + P[e^{-J_2} - 1]\,dG_2$$

Therefore,

$$\frac{dP}{P} = [-\alpha + \frac{1}{2}\sigma^2]\,dt - \sigma\,dw + [e^{-J_1} - 1]\,dG_1 + [e^{-J_2} - 1]\,dG_2$$

Note the similarity with HJM [23] pg 82.

Extending the example to two periods

$$\begin{aligned} df_1 &= \alpha_1 dt + \sigma_1 dw + J_1 dG_1 + J_2 dG_2 \\ df_2 &= \alpha_2 dt + \sigma_2 dw + J_1 dG_1 + J_2 dG_2 \end{aligned}$$

and

$$P(f_1, f_2) = e^{-f_1 - f_2}$$

Then

$$dP = -P([\alpha_1 + \alpha_2]\,dt + [\sigma_1 + \sigma_2]\,dw) + \frac{1}{2}[\sigma_1 + \sigma_2]^2 P\,dt + P[e^{-2J_1} - 1]\,dG_1 + P[e^{-2J_2} - 1]\,dG_2$$

Therefore,

$$\frac{dP}{P} = [-\sum_{i=1}^{2}\alpha_i + \frac{1}{2}(\sum_{i=1}^{2}\sigma_i)^2]\,dt - \sum_{i=1}^{2}\sigma_i\,dw + [e^{-\sum_{i=1}^{2}J_1} - 1]\,dG_1 + [e^{-\sum_{i=1}^{2}J_2} - 1]\,dG_2$$

Taking the limiting case where we get a series of instantaneous forward rates $f(t,s)$ for $s \in [t,T]$ we get the expression (6) in the paper:

$$\begin{aligned}
\frac{dP(t,T)}{P(t,T)} &= [a(t,T) + \frac{1}{2}b(t,T)^2]\,dt + b(t.T)\,dW_1(t) \\
&\quad +[e^{-J_1(T-t)} - 1]\,dG_1(t) + [e^{-J_2(T-t)} - 1]\,dG_2(t) \\
a(t,T) &= -\int_t^T \alpha(t,v)\,dv \\
b(t,T) &= -\int_t^T \sigma(v)\,dv
\end{aligned}$$

A.4 Programming Code for the Poisson-Gaussian Model

The program below is written in *Mathematica*.

```
(***-------------------------------------------------------***)
(*** HJM Model for Jump-diffusions - With Mean Reversion ***)
(***        Sanjiv Das, Harvard Business School          ***)
(***              copyright, April 1995                  ***)
(***-------------------------------------------------------***)
Step[x_]:=Block[{s},
        s=1; While[x>s*(s+1)/2,s=s+1]; Return[s];
        ]

T=3; h=0.5;
f0=Table[0.05+0.01*i,{i,T}];
beta=0.1; basesig=0.005;
sigma=Table[basesig*Exp[-beta*(t-1)],{t,T}]; sigma=sigma*Sqrt[h];
mu=0.0;
gamma=0.01;
lambda=0.1; lambda=lambda*h;

jumpshft=Table[0,{t,T},{i,t*(t+1)/2}];
For[t=2,t<=T,t++,
   For[i=1,i<=t*(t+1)/2,i++,
        If[i<=(t-1)*t/2,jumpshft[[t,i]]=jumpshft[[t-1,i]]+mu+gamma];
        If[i==(t-1)*t/2+1,jumpshft[[t,i]]=0];
        If[i>(t-1)*t/2+1,jumpshft[[t,i]]=(i-(t-1)*t/2-1)*(mu-gamma)];
        ];
   ];

(***** Risk Neutral Drifts *****)
alpha=Table[0,{t,T},{i,T-t+1}];
For[t=2,t<=T,t++,
   For[k=1,k<=T-t+1,k++,
        If[k==1,
           alpha[[t,k]]=Log[Exp[h*(-sigma[[t]]-mu-gamma)]*lambda/4+
                Exp[h*(-sigma[[t]])]*(1-lambda)/2+
                Exp[h*(-sigma[[t]]-mu+gamma)]*lambda/4+
                Exp[h*(sigma[[t]]-mu-gamma)]*lambda/4+
                Exp[h*(sigma[[t]])]*(1-lambda)/2+
                Exp[h*(sigma[[t]]-mu+gamma)]*lambda/4 ]/h,
           alpha[[t,k]]=Log[
```

```
                Exp[(-Sum[sigma[[t+j-1]],{j,k}]/k-mu-gamma)*h*k]*lambda/4+
                Exp[(-Sum[sigma[[t+j-1]],{j,k}]/k)*h*k]*(1-lambda)/2+
                Exp[(-Sum[sigma[[t+j-1]],{j,k}]/k-mu+gamma)*h*k]*lambda/4+
                Exp[(Sum[sigma[[t+j-1]],{j,k}]/k-mu-gamma)*h*k]*lambda/4+
                Exp[(Sum[sigma[[t+j-1]],{j,k}]/k)*h*k]*(1-lambda)/2+
                Exp[(Sum[sigma[[t+j-1]],{j,k}]/k-mu+gamma)*h*k]*lambda/4]/h
                - Sum[alpha[[t,i]],{i,k-1}] ];
        ];
   ];

(***** Forward Rate Tree *****)
f=Table[Table[0,{k,T-t+1}],{t,T},{i,t^2*(t+1)/2}];
f[[1,1]]=f0;
For[t=2,t<=T,t++,
   For[n1=1,n1<=t,n1++,
      For[n2=1,n2<=t*(t+1)/2,n2++,
         For[k=1,k<=T-t+1,k++,
            f[[t,(n1-1)*t*(t+1)/2+n2,k]]
                =f0[[t+k-1]]+Sum[alpha[[j,t+k-j]],{j,2,t}]
                        +sigma[[t+k-1]]*(t-1-(n1-1)*2)+jumpshft[[t,n2]];
            ];
         ];
      ];
   ];
r=Table[f[[t,i,1]],{t,T},{i,t^2*(t+1)/2}];

(***** Bond Pricing *****)
B=r; mat=T;
Do[B[[T,i]]=Exp[-h*r[[T,i]]],{i,T^2*(T+1)/2}];
For[t=mat-1,t>=1,t--,
   For[n1=1,n1<=t,n1++,
      For[n2=1,n2<=t*(t+1)/2,n2++,
         B[[t,(n1-1)*t*(t+1)/2+n2]]=Exp[-h*r[[t,(n1-1)*t*(t+1)/2+n2]]]*(
            B[[t+1,(n1-1)*(t+1)*(t+2)/2+n2]]*lambda/4+
            B[[t+1,(n1-1)*(t+1)*(t+2)/2+n2+Step[n2]]]*(1-lambda)/2+
            B[[t+1,(n1-1)*(t+1)*(t+2)/2+n2+Step[n2]+1]]*lambda/4+
            B[[t+1,n1*(t+1)*(t+2)/2+n2]]*lambda/4+
            B[[t+1,n1*(t+1)*(t+2)/2+n2+Step[n2]]]*(1-lambda)/2+
            B[[t+1,n1*(t+1)*(t+2)/2+n2+Step[n2]+1]]*lambda/4);
         ];
      ];
   ];
```

Table 1: **The Short Rate: Descriptive Statistics**
This table provides descriptive statistics on interest rate data at different frequencies. The data is the one-month T-bill rate. US dollar Monthly data spans the period January 1960 to December 1992. Weekly and Monthly data span the period January 1987 to December 1992. Weekly data is as of the last trading day of the week. Data have been obtained from Salomon Brothers and CRSP. Yen and Pound rates were obtained from Reuters, and are for a period of six years from 1989-94. Statistics are provided on the interest rates (r) as well as the changes in interest rates (dr). Raw data is in percentage terms.

Data Frequency	Mean	Variance	Skewness	Excess Kurtosis	No. of Obs
US$ Daily					1264
r	6.3615	1.5886	0.03474	-0.94064	
dr	-0.00057	0.072291	0.57903	17.3382	
US$ Monthly					396
r	5.9153	7.5614	1.0614	1.3207	
dr	-0.00169	0.6530	-0.8620	8.64524	
Yen Monthly					72
r	5.0167	4.4914	0.0950	-1.3985	
dr	-0.0291	0.0792	-0.0193	0.3209	
GB-Pound Monthly					72
r	10.0984	14.0039	-0.0980	-1.5600	
dr	-0.1007	0.1252	-0.6953	4.4023	

Table 2: **Number of Nodes in the Hexanomial Tree**

Number of Periods	Number of Nodes
1	6
2	18
3	40
4	75
5	126
10	726
15	2,176
20	4,851
30	15,376
50	67,626
100	520,251

Table 3: **Empirical Fit of the Constant Volatility Jump diffusion Model**
This table reports the fit of the Ho-Lee [25] jump diffusion enhanced model to U.K. gilt term structures and caps data. The term structure and caps go out to a maturity of 11 years and 10 years respectively. The volatility function uses a constant volatility parameter, i.e. $\sigma(T) = \sigma_0$. The average pricing error is reported as a measure of fit. The calibration was undertaken using a genetic algorithm. Fitting is undertaken each day for the cross section (across maturity) of interest rate securities.

Date	σ (bps)	λ (bps)	μ (bps)	γ (bps)	Average %age Pricing Error
01-Feb-95	154.96	0.4022	0.07	32.51	4.88
02-Feb-95	146.24	0.5134	16.12	2.27	5.13
03-Feb-95	129.47	0.6925	20.81	58.03	6.20

Table 4: **Volatility Term Structure from fitting the Black (1976) Model**
This table reports the volatility term structure from fitting the Black model to cap prices. The volatilities are reported for the five days of empirical investigation: 30-Jan-95 to 03-Feb-95. The volatilities are in percentage change per annum.

Maturity (yrs)	01-Feb-95	02-Feb-95	03-Feb-95
1	17.25	17.25	15.50
2	19.00	18.50	17.75
3	19.00	18.50	17.75
4	19.00	18.50	17.75
5	19.00	18.50	17.75
7	18.00	17.75	16.50
10	16.50	16.50	15.50

Table 5: **Empirical Fit of the Generalized Volatility Jump diffusion Model**
This table reports the fit of the generalized volatility jump diffusion enhanced model to U.K. gilt term structures and caps data. The term structure and caps go out to a maturity of 11 years and 10 years respectively. The volatility function uses a generalized term structure of volatilities, i.e.

$$\sigma(T) = A + B\exp(-T/D) + C\frac{T}{D}\exp(-T/D).$$

The average pricing error is reported as a measure of fit. The calibration was undertaken using a genetic algorithm. Fitting is undertaken each day for the cross section (across maturity) of interest rate securities.

Date	A	B	C	D	λ (bps)	μ (bps)	γ (bps)	Average %age Pricing Error
01-Feb-95	99.07	19.96	117.11	2.93	0.0612	27.32	131.11	2.02
02-Feb-95	93.61	15.30	166.81	2.73	0.0924	43.09	33.92	0.63
03-Feb-95	93.23	6.89	172.67	2.52	0.0506	21.08	0.01	0.83

Table 6: **Empirical Fit of the Generalized Volatility Model**
This table reports the fit of the generalized volatility model (without jumps) to U.K. gilt term structures and caps data. The term structure and caps go out to a maturity of 11 years and 10 years respectively. The volatility function uses a generalized term structure of volatilities, i.e.

$$\sigma(T) = A + B\exp(-T/D) + C\frac{T}{D}\exp(-T/D).$$

The average pricing error is reported as a measure of fit. The calibration was undertaken using a genetic algorithm. Fitting is undertaken each day for the cross section (across maturity) of interest rate securities.

Date	A	B	C	D	Average %age Pricing Error
01-Feb-95	109.04	2.77	145.36	2.75	2.26
02-Feb-95	111.50	14.22	106.12	3.53	2.81
03-Feb-95	137.22	-28.36	42.51	1.35	4.57

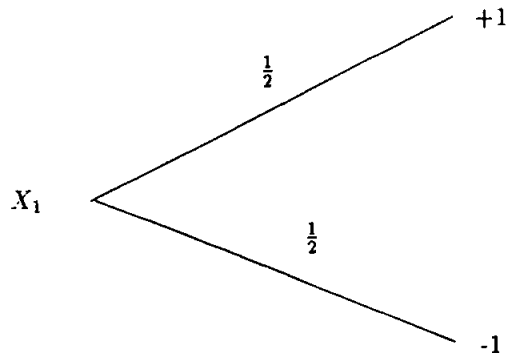

Figure 1: **Evolution of the Diffusion Random Variable**

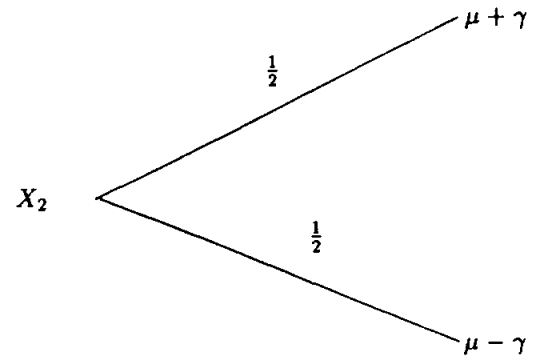

Figure 2: **Evolution of the Jump Random Variable**

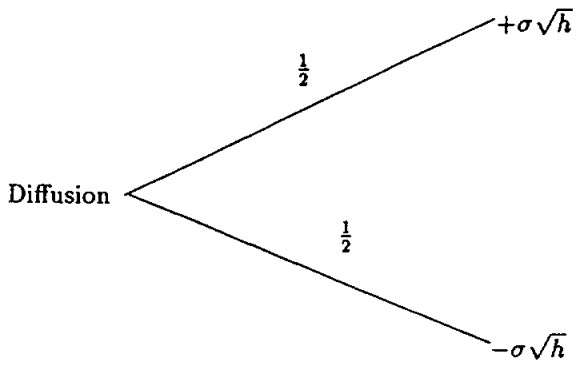

Figure 3: **Diffusion Shock**

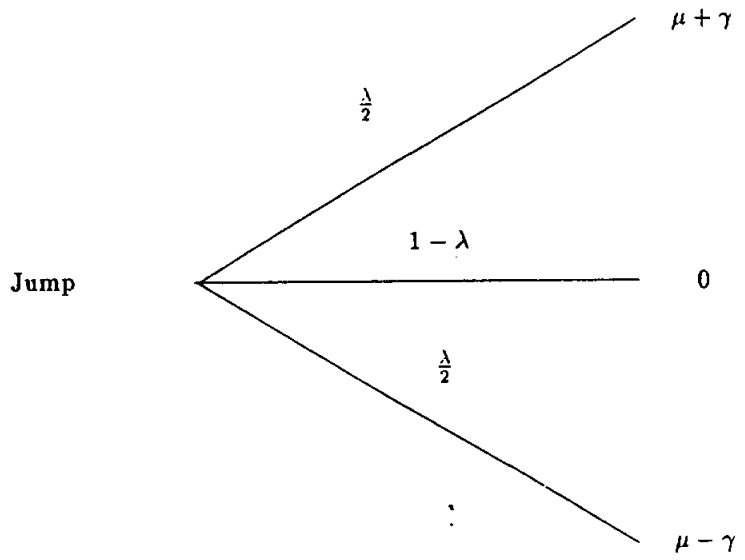

Figure 4: **Jump Shock**

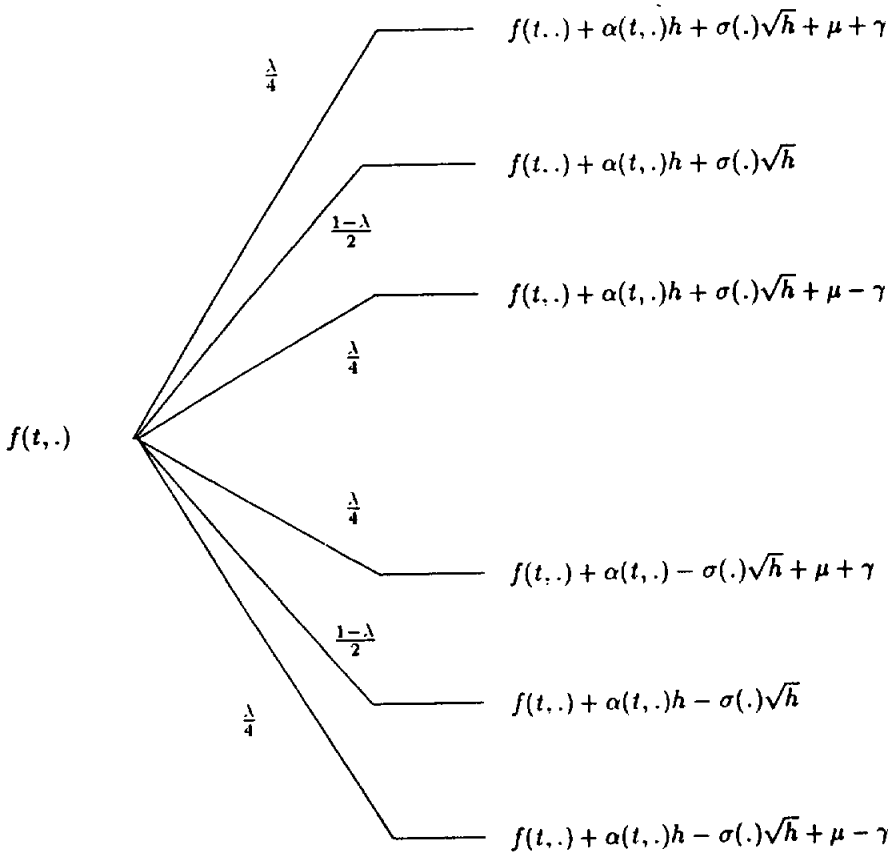

Figure 5: **Hexanomial Tree for the evolution of the Term Structure**

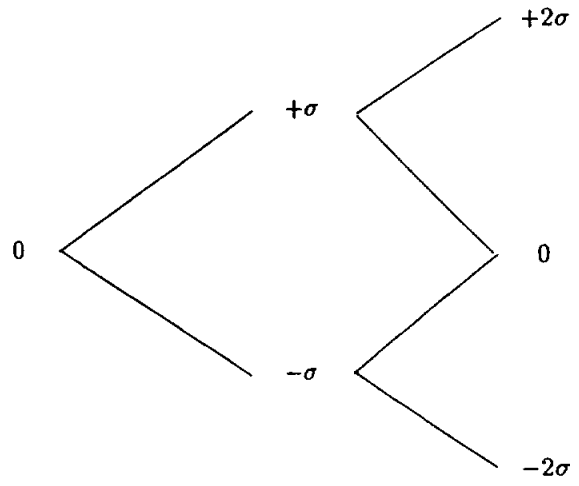

Figure 6: **Diffusion Space**

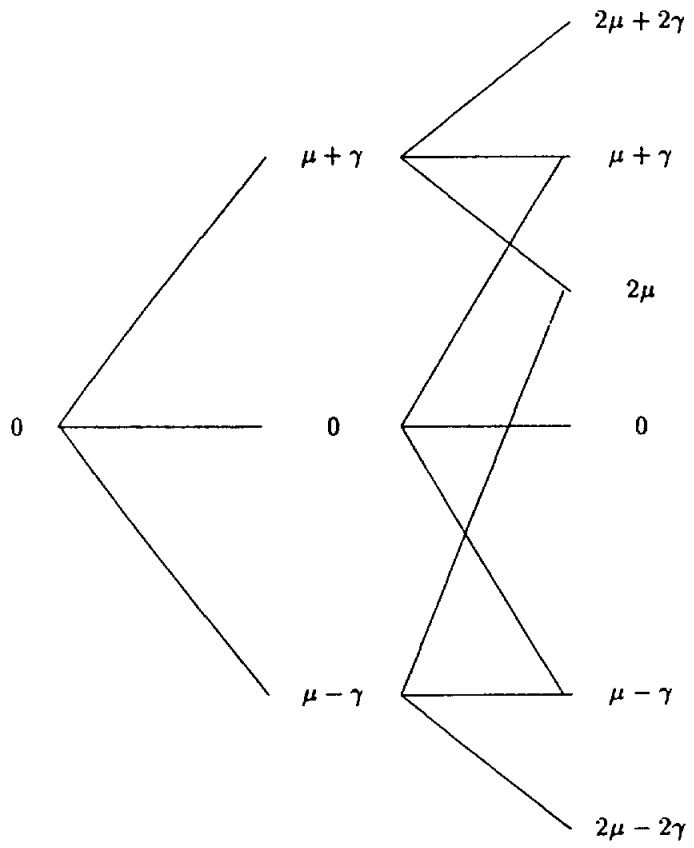

Figure 7: **Jump Space**

Figure 8: **Option Prices for varying Skewness - I**
Presented in this graph are European call option values for a 2.5-year option on a 5-year default free unit zero coupon bond. The plot presents values for skewness (μ) = -0.005, 0. 0.005. The instantaneous short rate (r_0) is varied from 5% to 15%. The exercise price is the at-the-money forward price of the underlying bond at option maturity. The forward rate curve used obeys the following function:

$$f(t) = r_0 + 0.01t$$

where t is the maturity of the instantaneous forward rate. The volatility parameter is $\sigma = 0.005$, the variance of the jump component is $\gamma^2 = 0.01^2$, volatility decay follows parameter $\beta = 0.1$, and jumps arrive at a rate determined by coefficient $\lambda = 0.1$.

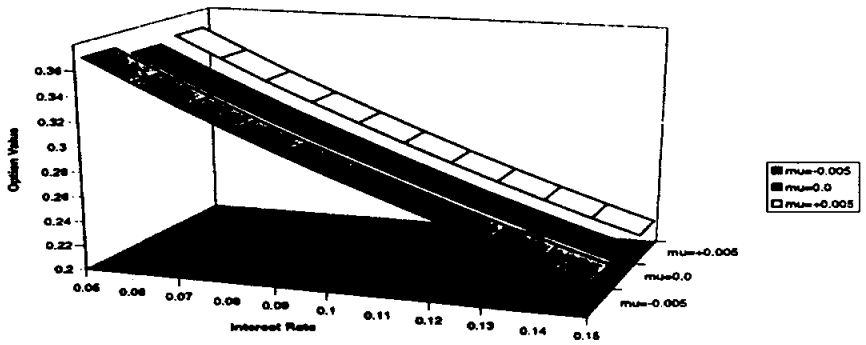

Figure 9: **Option Price Differences for varying Skewness - II**
Presented in this graph are differences in European call option values between a skewness and non-skewness model for a 3-year option on a 6-year default free unit zero coupon bond. There are two plots: one for the difference in value between the positive skewness model and the zero skewness model, and two, for the difference in value between the negative skewness model and the zero skewness model. The plot presents values for skewness (μ) = -0.01, 0.01. The instantaneous short rate (r_0) is varied from 5% to 15%. The exercise price is the at-the-money forward price of the underlying bond at option maturity for a short rate of 10% (i.e., the exercise price is \$72.33). The forward rate curve used obeys the following function:

$$f(t) = r_0 + \frac{\log(t)}{200}$$

where t is the maturity of the instantaneous forward rate. The volatility parameter is $\sigma = 0.005$, the variance of the jump component is $\gamma^2 = 0.01^2$, volatility decay follows parameter $\beta = 0.1$, and jumps arrive at a rate determined by coefficient $\lambda = 0.1$.

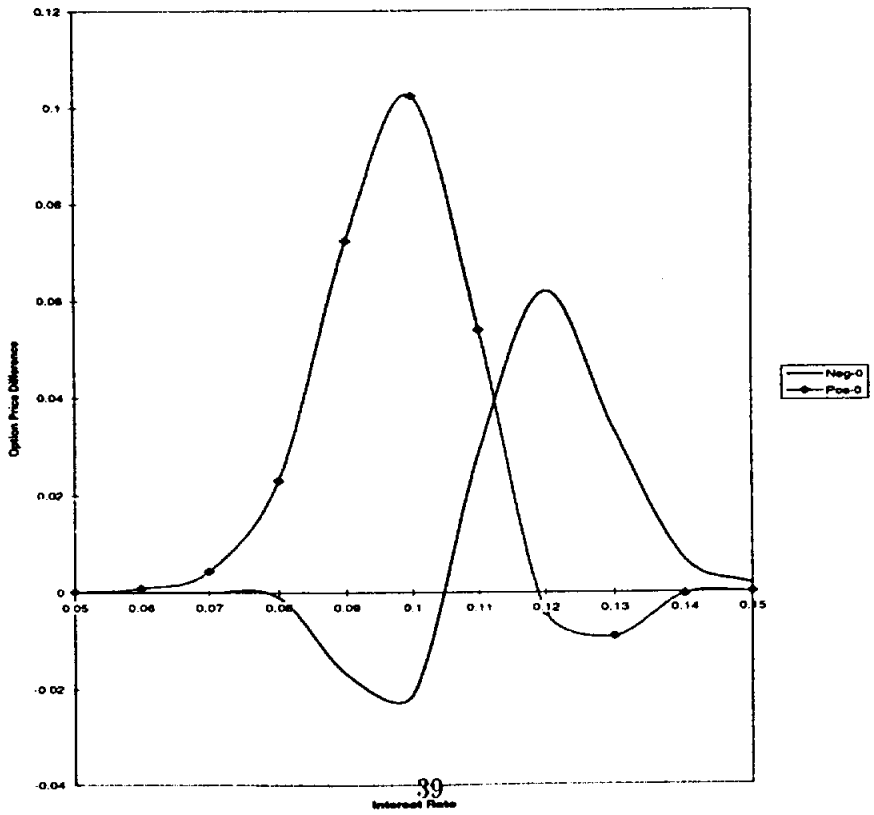

Figure 10: **Option Price Differences for varying Skewness - III**
Presented in this graph are differences in European call option values between a skewness and non-skewness model for a 5-year option on a 10-year default free unit zero coupon bond. There are two plots: one for the difference in value between the positive skewness model and the zero skewness model, and two, for the difference in value between the negative skewness model and the zero skewness model. The plot presents values for skewness (μ) = -0.01, 0.01. The instantaneous short rate (r_0) is varied from 5% to 15%. The exercise price is the at-the-money forward price of the underlying bond at option maturity for a short rate of 10% (i.e., the exercise price is \$57.60). The forward rate curve used obeys the following function:

$$f(t) = r_0 + \frac{\log(t)}{200}$$

where t is the maturity of the instantaneous forward rate. The volatility parameter is $\sigma = 0.005$, the variance of the jump component is $\gamma^2 = 0.01^2$, volatility decay follows parameter $\beta = 0.1$, and jumps arrive at a rate determined by coefficient $\lambda = 0.1$.

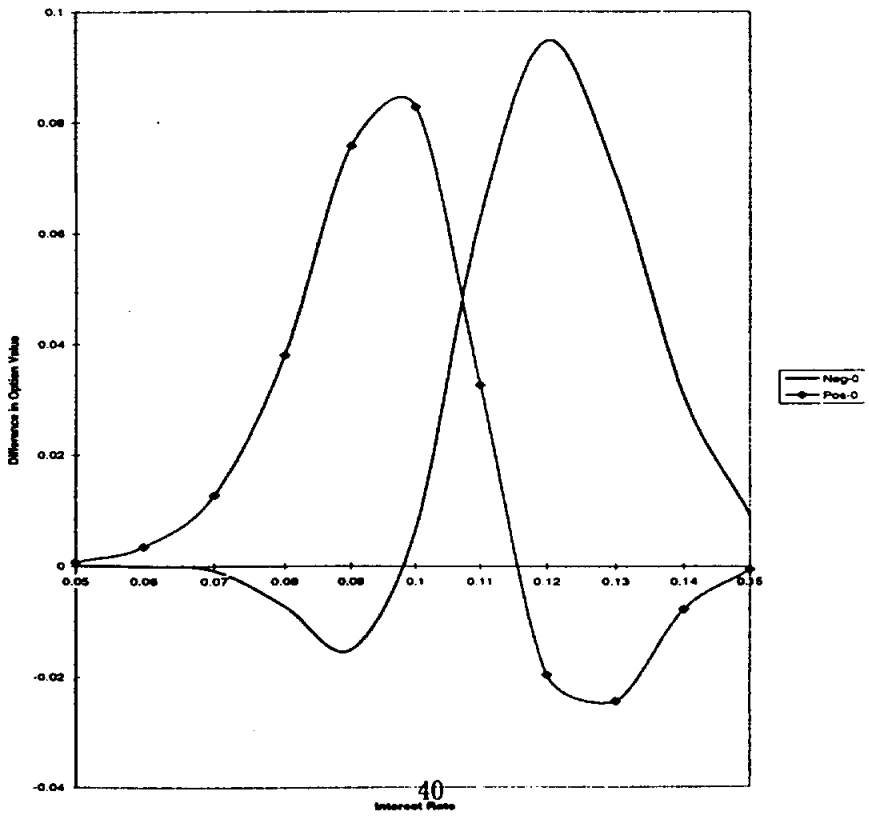

Figure 11: **Option Price Differences for varying Kurtosis - I**
Presented in this graph are the differences between Poisson-Gaussian and pure-Gaussian model prices for a 3-year European call option on a 6-year default free unit zero coupon bond. The plot presents values for kurtosis (γ) = 10, 60 and 110 basis points. The instantaneous short rate (r_0) is varied from 5% to 15%. The exercise price is the at-the-money forward price of the underlying bond at option maturity. The forward rate curve used obeys the following function:

$$f(t) = r_0 + \frac{\log(t)}{200}$$

where t is the maturity of the instantaneous forward rate. The volatility parameter is $\sigma = 0.005$, the mean of the jump component is $\mu = 0$, volatility decay follows parameter $\beta = 0.0$, and jumps arrive at a rate determined by coefficient $\lambda = 0.1$. In order to ensure consistency in the comparison of prices, the diffusion volatility is adjusted upwards to preserve the same level of total volatility per unit time as the Poisson-Gaussian model.

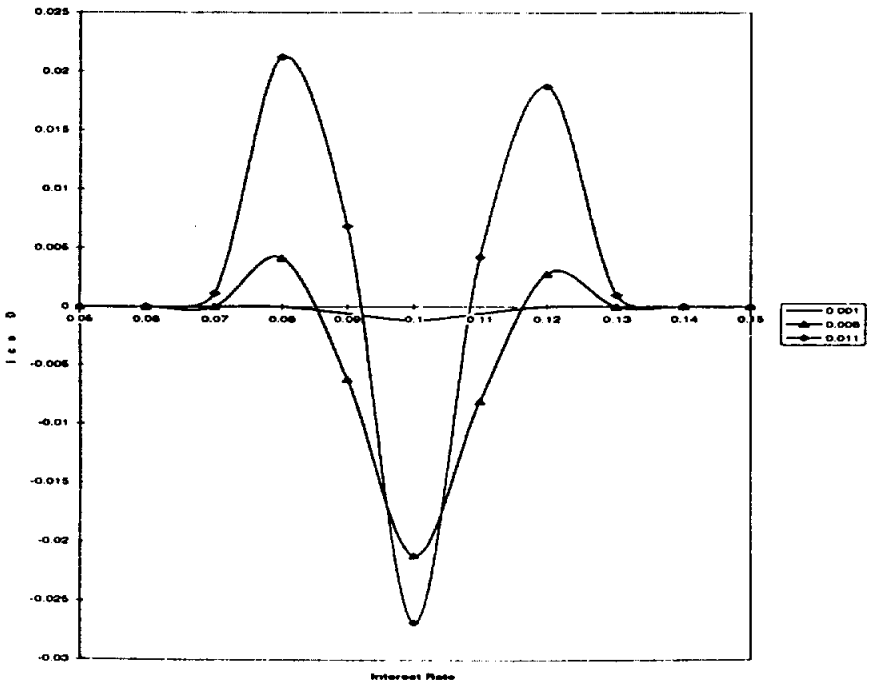

Figure 12: **Option Price Differences for varying Kurtosis - II**
Presented in this graph are the differences between Poisson-Gaussian and pure-Gaussian model prices for a 5-year European call option on a 10-year default free zero coupon bond. The plot presents values for kurtosis (γ) = 10, 60 and 110 basis points. The instantaneous short rate (r_0) is varied from 5% to 15%. The exercise price is the at-the-money forward price of the underlying bond at option maturity. The forward rate curve used obeys the following function:

$$f(t) = r_0 + \frac{\log(t)}{200}$$

where t is the maturity of the instantaneous forward rate. The volatility parameter is $\sigma = 0.005$, the mean of the jump component is $\mu = 0$, volatility decay follows parameter $\beta = 0.0$, and jumps arrive at a rate determined by coefficient $\lambda = 0.1$. In order to ensure consistency in the comparison of prices, the diffusion volatility is adjusted upwards to preserve the same level of total volatility per unit time as the Poisson-Gaussian model.